THE JOURNAL OF PHYSICAL CHEMISTRY A

 VOLUME 107, NUMBER 20, MAY 22, 2003

FEATURE ARTICLE

Structure, Bonding, and Vibrational Frequencies of CH_3CN-BF_3: New Insight into Medium Effects and the Discrepancy between the Experimental and Theoretical Geometries

David J. Giesen

Eastman Kodak Company, Building 83, Floor 2, RL, MC02216 Rochester, New York 14650-2216

James A. Phillips*

Department of Chemistry, University of Wisconsin−Eau Claire, 105 Garfield Ave., Eau Claire, Wisconsin 54702

Received: November 1, 2002; In Final Form: January 28, 2003

We have conducted an extensive computational study of the structure, bonding, B−N potential energy curve, and vibrational frequencies of CH_3CN-BF_3, using MP2, B3LYP, and BWP91 methods with basis sets ranging from STO-3G to aug-cc-pVQZ. Two types of minimum energy structures were found; one group with B−N distances near 1.8 Å, another with distances near 2.3 Å. In most cases, longer bond length structures were found with basis sets lacking diffuse functions, whereas shorter bond length structures were found when these functions were included. The exception is the largest basis set (aug-cc-pVQZ), for which the equilibrium B−N distance was found to be 2.315 Å. Potential energy curves calculated for the B−N stretching coordinate are found to be remarkably flat, and this results from the occurrence of two competing minima corresponding to the two types of minimum energy structures. At the B3LYP/aug-cc-pVQZ level, an extremely flat region occurs near 1.93 Å on the B−N potential curve, which lies about 0.2 kcal/mol above the global minimum after accounting for the effects of basis set super position error (BSSE) and zero-point vibrational energy (ZPE). The results are nearly converged with respect to basis set at the B3LYP/aug-cc-pVQZ level; further attempts at increasing the size of the basis set were not successful. An AIM analysis indicates that the two minima in the B−N potential arise from distinctly different interactions, the longer being primarily an electrostatic interaction, the inner being a partial covalent bond. Given the flat, asymmetric nature of the potential, it is very likely that the equilibrium and vibrationally averaged structures differ significantly due to large amplitude motion in the intermolecular B−N stretching mode. Furthermore, a comparison of experimental and calculated vibrational frequencies leads to the tentative conclusion that the B−N distance is significantly shorter in an argon matrix than in the gas phase.

I. Introduction

The structure and bonding of CH_3CN-BF_3 (acetonitrile−borontrifluoride) has been the study of numerous investigations over the past few decades. Even before the X-ray crystal structure was published in 1969,[1] some infrared bands had been measured in solution,[2] and a generalized normal coordinate analysis of CH_3CN-BX_3 species had been performed.[3] This earlier work culminated in a complete vibrational frequency analysis of the solid complex.[4] Recent interest arose when the

* To whom correspondence should be addressed. Phone: 715-836-5399. Fax: 715-836-4979. E-mail: phillija@uwec.edu

10.1021/jp022358i CCC: $25.00
Published on Web 04/11/2003

gas-phase structure of the complex was determined by FT microwave spectroscopy, and the complex was found to have a B−N distance of 2.011(7) Å and an N−B−F angle of 95.6-(6)°.[5] Surprisingly, these data suggested a donor−acceptor bond that defied classification as a purely "bonding" or "nonbonding" interaction, because the B−N distance and N−B−F angle were intermediate relative to values typical of a bona fide donor−acceptor adduct such as H_3N-BF_3, and weakly bonded complexes such as N_2-BF_3 and $NCCN-BF_3$. Specifically, H_3N-BF_3 has a 1.67(1) Å B−N distance in the gas phase, and the N−B−F angle of about 104°, indicating a near-tetrahedral geometry about the boron.[6] At the other extreme, N_2-BF_3[7] and $NCCN-BF_3$,[8] have B−N distances of 2.875(2) Å and 2.647(3) Å, respectively, and both have N−B−F angles near 90°, indicating that the BF_3 subunit remains essentially planar.

Not only was the gas-phase structure of CH_3CN-BF_3 peculiar in relation to analogous B−N complexes, it also differed markedly from the previously determined crystal structure, which had a B−N distance of 1.630(4) Å, and an N−B−F angle of 105.6(6)°.[1] Thus, upon crystallization, the donor−acceptor bond in CH_3CN-BF_3 contracts by nearly 0.4 Å, and the N−B−F angle opens by about 10°. These unusually large gas−solid structure differences have raised much interest in the effect of chemical medium on the structure of CH_3CN-BF_3, as well as a handful of other donor−acceptor species that have been shown to exhibit similar behavior.[9] In this spirit, several vibrational frequencies of CH_3CN-BF_3 were recently measured in an argon matrix,[10] and a comparison between these data and the frequencies of the crystalline complex[4] indicate that CH_3CN-BF_3 is significantly more weakly bonded in an argon matrix than in the solid state. Experimental gas-phase frequencies have yet to be measured, however, and in the absence of these data, the degree to which an argon matrix environment perturbs the structure and bonding of CH_3CN-BF_3 remains uncertain.

Given the myriad of intriguing experimental observations, it is no surprise that CH_3CN-BF_3 has also attracted the attention of computational chemists. However, all of the structural results published to date[11−15] agree quite poorly with experiment.[5] This is very unusual given the fact that CH_3CN-BF_3 contains only seven heavy atoms, and most of the computations were conducted at the MP2 level of theory with reasonably large basis sets. The first modern computational study, which aided initial searches for the microwave spectrum, predicted a 2.17 Å B−N bond length, an N−B−F angle of 98°, and a binding energy of −5.7 kcal/mol.[11] A few years later, Jonas, Frenking, and Reetz performed a comprehensive survey of 18 donor−acceptor complexes, and published a structure of CH_3CN-BF_3 with a B−N distance of 2.213 Å, an N−B−F angle of 95.8°, and a binding energy of −7.2 kcal/mol.[10] Shortly thereafter, as part of an effort to reproduce gas−solid structure differences using SCRF theory, Jaio and Schleyer reported a structure with a B−N distance of 2.277 Å, an N−B−F angle of 94.8°, and a binding energy of −7.0 kcal/mol.[13] These more recent results, though quite consistent with the first computational study, still predicted B−N distances that were about 0.2 Å longer than the experimental value. More recently, an MP2/6-31+G* structure was reported with a B−N distance of 1.801 Å,[14] just over 0.2 Å *shorter* than the experimental value. An N−B−F angle of 101.2°, a binding energy of −7.2 kcal/mol, and vibrational frequencies were also reported.[14] Despite the poor agreement with the experimental (gas phase) structure, the vibrational frequencies reported in that paper did compare favorably with matrix-IR frequencies.[10] Just last year, an HF/6-31G(d) structure was reported as part of a study attempting to parametrize the interaction energies in a series of BF_3 and SO_3 adducts.[15] However, the structural results reported for CH_3CN-BF_3 compared quite poorly with experiment, with a rather long 2.509 Å B−N distance and a 93.4° N−B−F angle.

Our initial motivation for the present study was to obtain credible ab initio frequencies for the gas-phase complex with which to compare matrix-IR results, and in turn, gauge the effect of an inert gas matrix on the structure and bonding of CH_3CN-BF_3. The first step was to obtain a reliable computational structure, and some simplistic frontier orbital considerations led us to suspect that some incorrect assumptions could have been made in the previous studies, and that they may be the underlying reason for the peculiar discrepancy between the experimental and the theoretical structures of the complex. Specifically, the HOMO of CH_3CN is an e − symmetry, π_{CN} − type orbital, though the σ_{CN} orbital is only about 0.6 eV lower in energy.[14,16] Of course, the LUMO of BF_3 is essentially an "empty p_z orbital" on the boron, with a small contribution from the p_z orbitals on the fluorines.[14] Thus, a simple, direct HOMO−LUMO interaction would render the complex bent about the C−N−B linkage. As best we can tell from the manuscripts,[11−15] geometry optimizations were constrained to C_{3v} in all of the previous computational studies. This was most certainly appropriate, given that the crystalline complex is clearly C_{3v}, and that the microwave spectrum was indicative of a 3-fold symmetric structure. However, there are a few cases, such as $HCl-BF_3$,[17] $HF-BF_3$,[18] and $OCO-BF_3$,[19] in which large amplitude vibrational motions render the complex symmetric on the microwave time scale, even though the true minimum energy structure is asymmetric. At the very least, an interaction between the π_{CN}-type HOMO of CH_3CN and the LUMO of BF_3 might result in a soft bending potential, and even if the equilibrium structure was not bent at relatively long B−N distances, perhaps large amplitude bending motions were obscuring the gas-phase structure analysis. Thus, our initial goal was to map a potential energy surface along both the B−N stretching and the C−N−B bending coordinates. Below, results from B3LYP[20] calculations will show that most of these initial suspicions were incorrect; the equilibrium structure appears to be C_{3v}, and the bending potential is not unusually flat. However, it was found that the intramolecular stretching potential is remarkably flat, and it appears that the discrepancy between the experimental and computational structures of CH_3CN-BF_3 may stem from a genuine difference between the equilibrium and vibrationally averaged geometries; the result of large amplitude vibrational motion along the B−N stretching coordinate. This observation motivated us to examine the nature of the bonding in the complex. Ultimately, we did obtain vibrational frequencies as well, and we will explore their structural dependence and compare them to experimental data for both crystalline and matrix-isolated CH_3CN-BF_3.

II. Computational Methods

All calculations were performed with *Gaussian 98* revision A.9.[21] Geometry optimizations used the opt = tight option which gives convergence thresholds of 1.5×10^{-5}, 1.0×10^{-5}, 6.0×10^{-5}, and 4.0×10^{-5} on the maximum force, RMS force, maximum displacement and RMS displacement, respectively. Without the opt = tight option, many calculations failed to find the true minimum geometry due to the flat nature of the B−N distance potential energy surface. Potential energy curves were computed by freezing the B−N distance at various values and optimizing all other degrees of freedom. Points on the curves

TABLE 1: Equilibrium B−N Distances (Å) of CH_3CN-BF_3 for Various Basis Sets

basis set	B3LYP	MP2
STO-3G	2.54	2.58
3-21G	1.76	1.85
Dz(d)[a]		2.17
6-31G(d)	2.28	1.88
6-31G(d,p)[b]		2.28
6-31+G(d)	1.75	1.75
6-31G(2d)	2.32	2.23
6-31+G(2d,p)	1.79	1.80
6-31G(3d)	1.82	1.82
6-31G(3df)	1.87	1.84
6-31G(3df,p)	1.87	1.84
6-31++G(3df,3pd)	1.85	1.82
6-311G(d)	2.33	2.37
6-311+G(d)	1.80	1.80
cc-pVDZ	2.07	
aug-cc-pVDZ	1.77	
TZ2P[c]	2.21	
cc-pVTZ	2.34	
aug-cc-pVTZ	1.87	
cc-pVQZ	2.34	
aug-cc-pVQZ	2.32	

[a] Double-ζ polarized basis set with diffuse functions on fluorine only. Basis set and results from ref 11. [b] Ref 13, gas phase. [c] Ref 12.

were computed every 0.05 Å from 1.5 to 2.4 Å as well as 2.5 and 2.6 Å. For the aug-cc-pVQZ surface, additional points were computed at 2.8, 3.0, and 3.5 Å.

III. Results and Discussion

Equilibrium Structures. Equilibrium structures (C_{3v}) obtained from MP2[22] and/or B3LYP calculations using a myriad of basis sets are summarized in Table 1, which shows only B−N distances as the other structure parameters have been omitted for clarity. It should be noted that stringent convergence criteria as detailed in the Computational Details section were needed to obtain these results. This was the first indication of an unusually flat intermolecular potential. The data in Table 1 seem to fall into two distinct groups; one with equilibrium B−N distances near 1.8 Å that agree well with ref 14, and the other with B−N distances near 2.3 Å, in fair agreement with refs 11−13. Neither group agrees well with the experimental value of 2.011 Å. Because the MP2 and B3LYP results are quite consistent for all but the smallest basis sets, the choice of computational method is apparently not the reason for the two distinct types of structures. Rather, it appears that basis sets augmented with diffuse functions (those basis sets with "+" or "aug" in the name) or d functions with unusually small exponents (those basis sets with "3d" in the name) favor the shorter bond length structure, whereas those that lack these functions favor the longer bond length structure. An exception to this separation is the aug-cc-pVQZ[23] result, which has a minimum energy structure with a 2.315 Å B−N distance, despite containing diffuse functions. Collectively, the results appear to show that the equilibrium geometry is not yet converged at the aug-cc-pVQZ level of theory, which is remarkable for a species of this size. However, as discussed below, when the calculations are corrected for basis set superposition error, it appears that the aug-cc-pVQZ results are nearly converged. Further increases in basis set size were unsuccessful due to computational limitations. Full geometries for the two most sophisticated models (B3LYP/aug-cc-pVTZ[23] and B3LYP/aug-cc-pVQZ) are shown in Figure 1. The binding energy is −5.1 kcal/mol at the B3LYP/aug-cc-pVQZ level, as calculated from the difference in electronic energies between the complex and the isolated

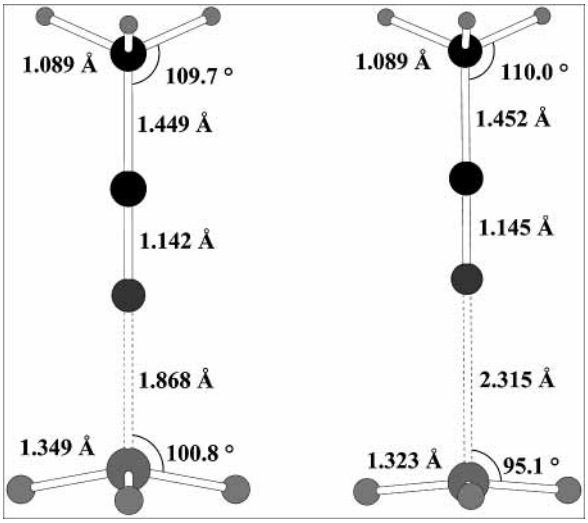

Figure 1. Equilibrium Structures of CH_3CN-BF_3 calculated at the B3LYP/aug-cc-pVTZ (left) and B3LYP/aug-cc-pVQZ (right) levels of theory.

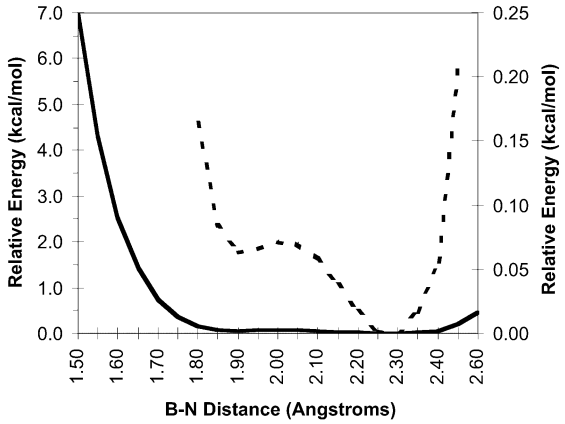

Figure 2. Potential energy (electronic) of CH_3CN-BF_3 versus B−N distance, calculated at the B3LYP/6-31G(d) level of theory. The solid line shows the full potential energy surface and corresponds to the left-hand *Y*-axis. The dashed line is a blow-up of the flat portion of the surface and corresponds to the right-hand *Y*-axis.

reactants. In any event, the collection of results in Table 1 do explain, at least in a phenomenological sense, the reason behind the disagreement between the previously reported MP2 theoretical structures.[11−14] In ref 14, a 6-31+G* basis was used and a B−N distance of 1.80 Å was found, whereas the others used double-ζ basis sets lacking diffuse functions on B and N and found longer bond lengths between 2.17 and 2.28 Å. This distinction between augmented and nonaugmented basis sets also provides an alternative explanation to the condensed phase results in ref 13, where a large decrease in bond length was found between computed gas phase and SCRF structures. However, the gas-phase results were computed with a nonaugmented basis set and the SCRF structure was computed with an augmented basis set, and the decrease in bond length from 2.28 Å to 1.65 Å is only slightly greater than the difference between augmented and nonaugmented basis sets in Table 1.

B−N Distance Potential. The reasons underlying these unusual structural results become much more apparent upon examination of the potential energy along the B−N stretching coordinate. Figure 2 shows a B−N potential curve (constrained to C_{3v}) calculated at the B3LYP/6-31G(d)[24] level of theory. The immediately striking feature is that the curve is extremely flat and remains under 1.0 kcal/mol for over 1.0 Å, and under 0.1 kcal/mol from 1.85 Å to 2.35 Å; this essentially spans both

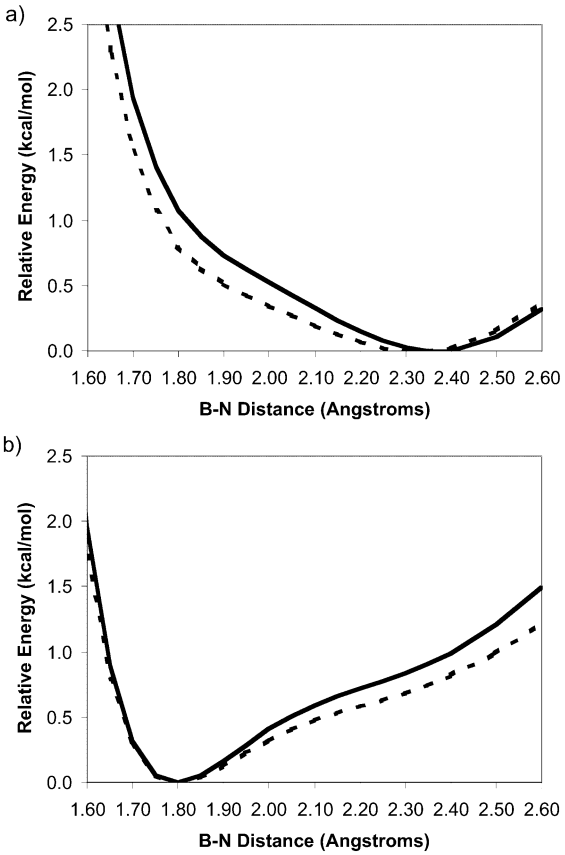

Figure 3. (a, top) Potential energy (electronic) of CH_3CN-BF_3 versus B−N distance calculated with the MP2 method (solid) and the B3LYP method (dashed) using the 6-311G(d) basis set. (b, bottom) Potential energy of CH_3CN-BF_3 versus B−N distance calculated with the MP2 method (solid) and the B3LYP method (dashed) using the 6-311+G(d) basis set.

types of B−N distances noted above. The flatness appears to be the result of two competing minima, one corresponding to each type of structure noted above. Because these results were obtained with a basis set lacking diffuse functions, the longer minimum is lower in energy. Clearly such a potential would allow for very large amplitude vibrational motions along the B−N bond, even in the ground vibrational state. The experimental B−N distance of 2.011 Å happens to lie near the center of the flat region of the curve; about 0.3 Å shorter than the global minimum. If the true potential energy surface has this asymmetrical shape, a large amplitude B−N stretching motion would cause a significant difference between the equilibrium and vibrationally averaged bond lengths.

B−N potential curves obtained with larger basis sets are shown in Figure 3. The upper panel (a) shows curves (MP2 and B3LYP) obtained with the 6-311G(d)[25] basis set, and the lower panel shows curves for the 6-311+G(d)[25] basis set. Because the only difference between the two basis sets in 3a and 3b are the diffuse ("+") functions on heavy atoms, these curves illustrate the effect of the functions on the equilibrium B−N distance as described above. Although each of these curves has only a single minimum, each also has a "plateau-like" feature in the region of the second minimum found in Figure 2. Specifically, in 3a, the absence of diffuse functions in the 6-311G(d) basis set favors the longer bond length minimum (∼2.3 Å), but there are clear indications of a flattened region around 1.9 Å. Conversely, the curves in Figure 3b, obtained using the 6-311G+(d) basis, have a true minimum near 1.8 Å and a flattened region near 2.3 Å. Despite the shoulder features, these curves lack the flatness needed to rationalize any consistency with the experimental bond length. However, the B−N bond potential is clearly not converged with respect to basis set in Figure 3, so larger basis sets were tried. Because of the similarity of the B3LYP and MP2 results shown in Table 1 and Figure 3, only B3LYP was used for the remainder of the analysis presented below.

Figure 4 displays B−N potential curves calculated at the B3LYP/aug-cc-pVTZ and B3LYP/aug-cc-pVQZ levels of theory. Again, the striking feature of both curves is the extensive flat

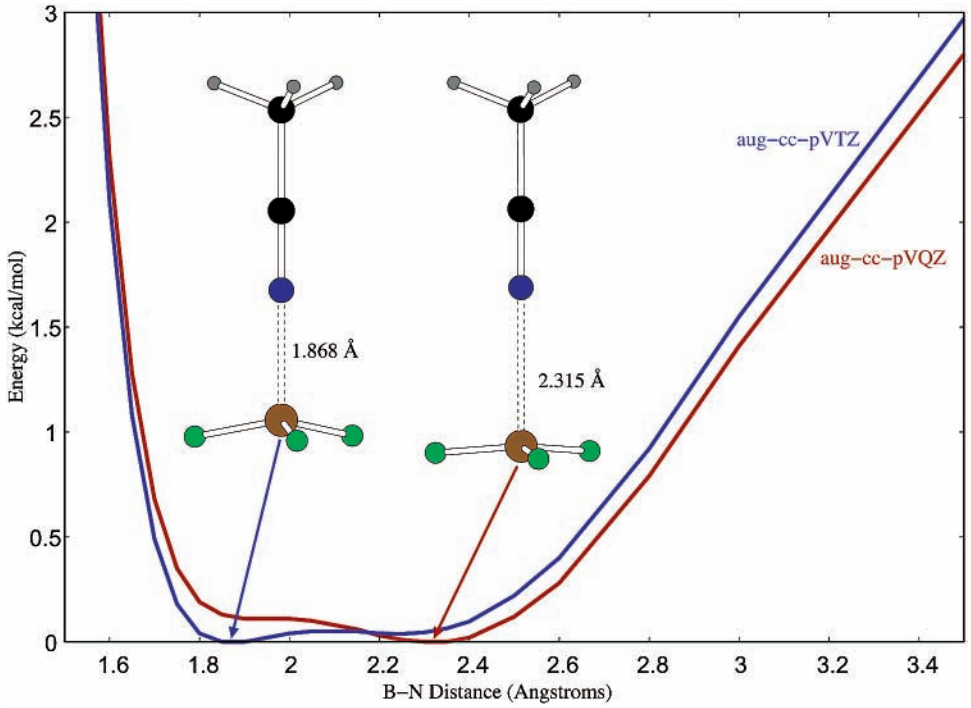

Figure 4. Potential energy (electronic) of CH_3CN-BF_3 versus B−N distance calculated with at the B3LYP/aug-cc-pVTZ level (blue) and the B3LYP/aug-cc-pVQZ level (red).

TABLE 2: Experimental and B3LYP/Aug-cc-pVQZ Vibrational Frequencies (cm^{-1}) for CH_3CN, $^{11}BF_3$, and the $CH_3CN-^{11}BF_3$ Complex

mode	reactant expt[a]	reactant calc[b]	complex sym.	complex 2.315 Å	complex 1.919 Å	complex Ar matrix[c]	complex crystal[d]	approximate description
ν_1	2954	2925	A_1	2928	2929		2956	CH_3 sym. str.
ν_2	2262	2268	A_1	2295	2324	2365	2376	C−N str.
ν_3	1390	1415	A_1	1414	1413		1372	CH_3 umbrella
ν_4	920	928	A_1	938	951		978	C−C str.
ν_5			A_1	63	47		359[e]	B−N str.
ν_6	888	884	A_1	859	830	858[f]	894	BF_3 sym str.
ν_7	691	684	A_1	587	564	601	657[e]	BF_3 umbrella
ν_8			A_2	20	22			Torsion
ν_9	3009	2991	E	2996	3000		3030	CH_3 asy. str.
ν_{10}	1448	1475	E	1472	1468		1430	CH_3 asy. def.
ν_{11}	1041	1063	E	1063	1062		1031	CH_3 rock
ν_{12}	365	380	E	396	412		423	N−C−C bend
ν_{13}	1453	1441	E	1395	1306	1249	1198	BF_3 asy. str.
ν_{14}	480	475	E	474	487		521	BF_3 asy. def.
ν_{15}			E	187	266		314	BF_3 rock
ν_{16}			E	42	59			B−N−C bend

[a] Reference 28 for acetonitrile frequencies and Reference 29 for BF_3 frequencies. [b]Frequencies higher than 2000 cm^{-1} have been scaled by 0.96. See text for discussion. [c]Reference 10. [d]Reference 4. [e]The solid-state assignments for ν_5 and ν_7 have been switched, as suggested by Reference 14, see text for discussion. [f]Assignment is tentative. It should be noted that three distinct absorption features were observed between 820 and 855 cm^{-1}, and none of these could be confirmed or excluded as assignments for ν_6.

region that is apparently the result of the two competing interactions, one that is optimal near 1.8 Å and one near 2.3 Å. The aug-cc-pVTZ curve is remarkably flat, and remains at or below 0.05 kcal/mol (17 cm^{-1}) from 1.8 Å to 2.4 Å. The inner minimum at 1.87 Å is global, the secondary minimum lies at 2.25 Å, and the barrier between the two is only 0.05 kcal/mol (17 cm^{-1}) relative to the global minimum. The aug-cc-pVQZ curve is also quite flat, but shows a clear preference for the outer minimum. The curve remains below 0.15 kcal/mol (52 cm^{-1}) from about 1.8 to 2.5 Å. The global minimum is at a B−N distance of 2.315 Å. An extremely shallow minimum with no imaginary frequencies that lies 0.11 kcal/mol higher than the global minimum is found at 1.919 Å, with a barrier less than 0.001 kcal/mol toward longer B−N distances. Again, neither global minimum agrees well with the experimental B−N distance of 2.011 Å, but this vibrationally averaged bond length does lie well within the flat region of the potential. Furthermore, the peculiar asymmetric shape of these curves would most certainly result in a significant difference between the equilibrium and vibrationally averaged bond lengths. At this point, we can qualitatively rationalize some consistency with experiment, because the potential near the global minimum on the aug-cc-pVTZ curve is much softer along the inner wall, which would make the vibrationally averaged B−N distance *shorter* than the global minimum; toward the experimental value of 2.01 Å. Moreover, given that the barrier between the minima is so low, even a modest zero point energy of 0.1 kcal/mol in the B−N stretching mode would correspond to classical turning points separated by about 0.6 Å. In turn, this would have the complex sweeping through a range of B−N distances in a single vibrational period that almost spans those characteristic of both moderately strong donor acceptor adducts and weakly bonded complexes! Although we have no reliable assessment of the zero-point energy or vibrational amplitude in the B−N stretching coordinate at this point, the calculated (harmonic) B−N stretching frequency (Table 2) suggests that the ground vibrational level would lie very near the shelf-like, secondary minimum in the aug-cc-pVQZ curve. The simplistic harmonic estimates we have made by fitting various regions of the aug-cc-pVQZ curve to a force constant are consistent with this, as we estimate a zero point energy of 0.14 kcal/mol (48 cm^{-1}) from a set of points near the global minimum, and a value of 0.10 kcal/mol (34 cm^{-1}), from a (quite poor) fit of the entire well. A full rationalization of the experimental bond length will not only require a sophisticated, anharmonic treatment of the ground state vibrational energy, and also a curve that is fully converged with respect to basis set and quite accurate in the 1.9 Å region. At this point, however, it seems quite likely that there is a significant difference between the equilibrium and vibrationally averaged B−N bond distances, and that the latter should be significantly shorter. In turn, these data suggest that the peculiar discrepancy between the theoretical and experimental structures of the complex may indeed be genuine.

With potential energy curves this flat, it is possible that sometimes-overlooked effects such as basis set superposition error (BSSE) and zero-point energy (ZPE) could have a large effect on the equilibrium B−N distance. The counterpoise correction[26] was used to estimate the amount of BSSE in the distance potential curves. The procedure at a given B−N distance used the following steps: (1) compute the energy and geometry of the complex with a frozen B−N distance ($E_{complex}$), (2) compute the energy of acetonitrile (ACN) at the complex geometry (E_{ACN}), (3) compute the energy of ACN at the complex geometry in the presence of BF_3 ghost functions at the BF_3 complex geometry ($E_{ACN(gh)}$), (4) compute the energy of BF_3 at the complex geometry (E_{BF3}), and (5) compute the energy of BF_3 at the complex geometry in the presence of ACN ghost functions at the ACN complex geometry ($E_{BF3(gh)}$). The estimate of the BSSE-corrected energy (E_{Corr})at that B−N distance is then given by

$$E_{coor} = E_{complex} + (E_{ACN} + E_{BF3} - E_{ACN(gh)} - E_{BF3(gh)}) \quad (1)$$

As shown in Figure 5, the BSSE correction is quite large for small- to medium-sized basis sets. In all cases, there is a destabilization of the shorter minimum. The 6-31G(d) potential is no longer flat and the global minimum has moved about 0.2 Å longer. The shorter minimum has become little more than a shoulder on the curve. The medium-sized basis sets with diffuse functions in Figure 5b have very similar looking curves. After the BSSE correction, the 6-311+G(d) and the aug-cc-pVDZ[23] curves appear almost identical. Although the strongly favored short minimum remains the only minimum for these basis sets and shifts only slightly longer, the shoulder at the longer distance

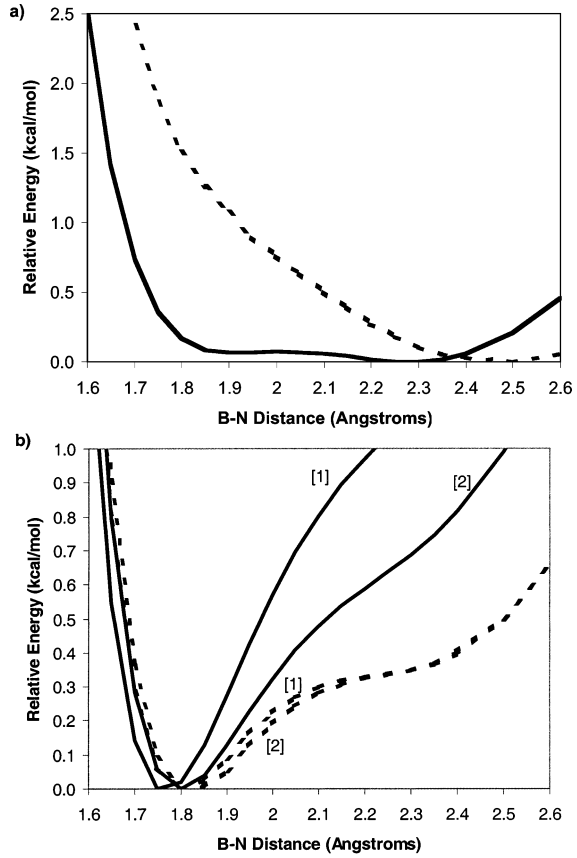

Figure 5. BSSE-corrected (dashed) and uncorrected (solid) potential energy surfaces. (a, top): B3LYP/6-31G(d), (b, bottom): B3LYP/aug-cc-pVDZ [1] and B3LYP/6-311+G(d) [2].

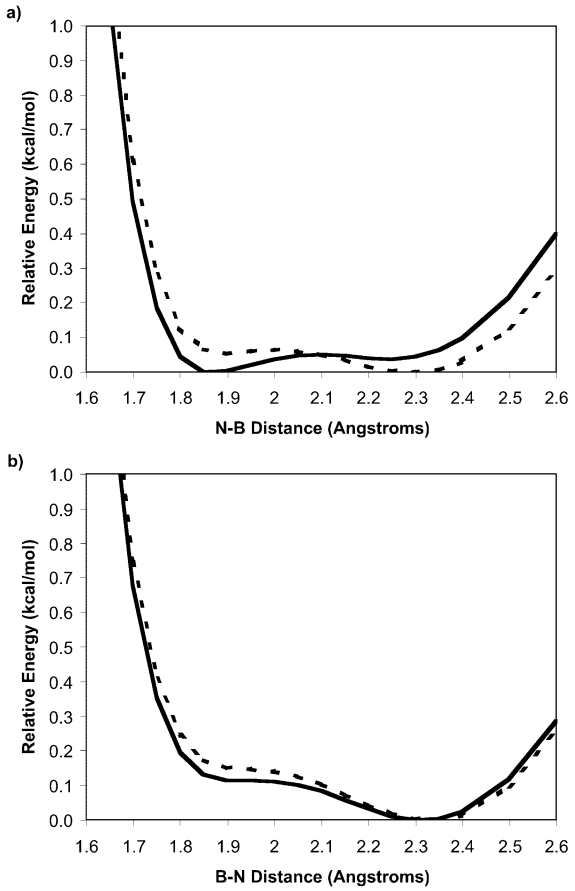

Figure 6. BSSE-corrected (dashed) and uncorrected (solid) potential energy surfaces. (a, top): B3LYP/aug-cc-pVTZ, (b, bottom): B3LYP/aug-cc-pVQZ.

has become much more pronounced. Figure 6 shows the effect of the BSSE correction on the large aug-cc-pVTZ and aug-cc-pVQZ basis sets. The BSSE correction is much smaller for these two basis sets. However, it is enough to qualitatively change the aug-cc-pVTZ curve to favor the longer minimum, so that the BSSE counterpoise correction changes the equilibrium bond length by 0.4 Å. The effect on the aug-cc-pVQZ potential energy surface is trivial. By using the BSSE correction, convergence in basis set size is nearly achieved. Not only is the BSSE correction trivial for aug-cc-pVQZ, but also the BSSE-corrected relative energy curves for aug-cc-pVTZ and aug-cc-pVQZ differ by less than 0.14 kcal/mol over the entire span of B−N distances from 1.5 to 2.6 Å.

With very large BSSE corrections and qualitatively incorrect results for basis sets smaller than aug-cc-pVTZ, any properties of this complex calculated with smaller basis sets are dubious and probably meaningless. Unfortunately, this rules out using higher-level methods such as MP4, CISD, or QCISD with available computational resources. Without resorting to these higher level methods, it is difficult to check the validity of the B3LYP results. In an effort to perform some consistency check, the pure DFT method BPW91[20a,27] was used with several basis sets. The resulting B−N distance potentials are shown in Figure 7. The BPW91/6-311G(d) and BPW91/6-311+G(d) curves (a and b) can be compared to the B3LYP and MP2 curves in Figure 3a and 3b. From this, it is seen that BPW91 strongly favors the short minimum compared to the other two methods. It is not surprising then, that the BPW91/aug-cc-pVQZ curve also favors the short minimum over the long minimum, in contrast to B3LYP/aug-cc-pVQZ. All the curves do clearly show a "plateaulike" region near the 2.3 Å minimum as well, and they (like

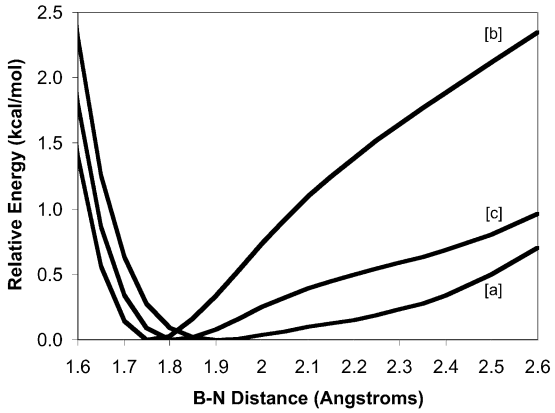

Figure 7. Potential energy (electronic) of CH_3CN-BF_3 versus B−N distance calculated with the BPW91 method using the [a] 6-311G(d), [b] 6-311+G(d), and [c] aug-cc-pVQZ basis sets.

the B3LYP curves in Figure 3) also lack the flatness to rationalize any agreement with the experimental structure. One difficulty with DFT is that when two methods disagree, there is no a priori way to tell which one is more reliable. However, in this case the close agreement between B3LYP and MP2 provides good confidence in the B3LYP results, and the B3LYP method will be used for further analysis.

The zero-point energy can be evaluated for each minimum using the computed frequencies. Harmonic vibrational frequencies from ab initio and density functional theory calculations are typically multiplied by empirically established scale factors when comparing to experimental frequencies.[28] To determine an appropriate scale factor for the B3LYP/aug-cc-pVQZ cal-

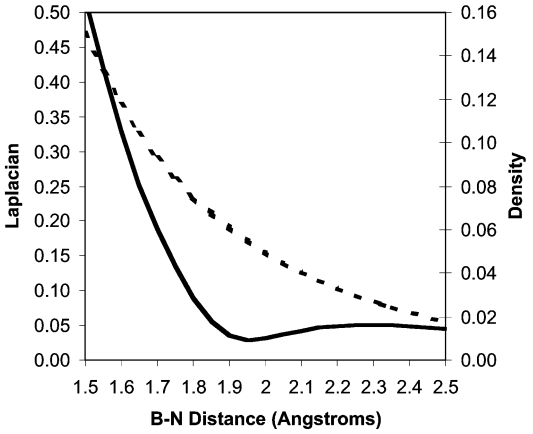

Figure 8. Electron density (dashed) and Laplacian of the electron density (solid) at the B−N bond critical point by AIM analysis.

culations, computed frequencies for the isolated acetonitrile and borontrifluoride molecules were compared to gas-phase experimental frequencies.[29,30] Although the typical scale factor for B3LYP calculations is about 0.96,[28] it was found that frequencies below 2000 cm^{-1} agreed well with experiment without any scale factor. For frequencies above 2000 cm^{-1}, a scale factor of 0.96 gave good agreement with the experimental frequencies. Because one of the goals of this work is to obtain computed frequencies useful in interpreting experimental measurements, the following method was adopted for scaling computed frequencies of the CH_3CN-BF_3 complex: frequencies above 2000 cm^{-1} were scaled by 0.96 and frequencies below 2000 cm^{-1} were left unscaled. This scheme gives an RMS difference of 17 cm^{-1} between the calculated and experimental frequencies for acetonitrile and borontrifluoride, and the results are shown in Table 2. Frequencies for the complex were calculated at the two minima on the B3LYP/aug-cc-pVQZ potential energy curve and are also shown in Table 2. The difference in ZPE (arising from modes other than the B−N stretch) between the two minima favors the longer minimum by 0.09 kcal/mol. This raises the difference in energy between the two minima to 0.20 kcal/mol.

Bonding. Because the potential energy surface indicates that the ground state vibrational amplitude may sweep through regions that vary widely in bonding character, an analysis of the bonding along the B3LYP/aug-cc-pVQZ potential energy surface was completed using the Atoms in Molecules[31] (AIM) approach. The density at a bond critical point in the AIM methodology can be related to the strength of the bonding interaction, and the sign of the Laplacian of the electron density at the critical point gives information as to the type of bonding interaction.[32] A positive Laplacian is associated with so-called "closed shell" interactions such as hydrogen bonds, noble gas dimers and ionic bonds.[32] A negative Laplacian is associated with covalent bonding.[32] Figure 8 shows both the density and the Laplacian of the density as a function of the B−N distance for B3LYP/aug-cc-pVQZ calculations. At the minimum energy distance of 2.32 Å, the density has a value of 0.026. This value is similar to those found for hydrogen bonds.[32,33] In the shelf region at 1.9 Å, the density has doubled to 0.061. This is about twice as large as the value for most hydrogen bonds, but it still considerably smaller than the value for a typical single bond, many of which have density values between 0.20 and 0.30.[33] The Laplacian has several interesting features. The first feature is a local maximum that appears at about 2.3 Å. Because a positive Laplacian is associated with electrostatic interactions, this is consistent with the picture that the long minimum is a result of electrostatic attraction. The second interesting Laplacian feature is the local minimum at 1.95 Å. Although the Laplacian never becomes negative, this dip indicates an increasingly covalent character to the B−N interaction and is consistent with the idea that the short minimum results from the formation of a weak partial bond. The occurrence of two distinct minima arising from different interactions is quite significant. First of all, large amplitude motion in the B−N stretching coordinate would apparently have the partial bond forming and breaking in the course of a vibrational period. Furthermore, the effect of chemical medium on the structure of CH_3CN-BF_3 and other complexes with partial bonds has been previously rationalized primarily from the standpoint that only a single minimum exists, and that it is shifted via interactions with the surrounding environment.[5,9,34] The present results indicate that the structure is quite sensitive to a delicate energetic balance between *two* minima along the B−N potential, and it is quite likely that environmental effects would significantly disrupt this balance (see below). Although either an AIM or Natural Bond Orbital analysis of the B−N bond order would be interesting, neither method was able to successfully complete using either the aug-cc-pVTZ or aug-cc-pVQZ basis set using the G98 program. Both the Mulliken and the Löwdin bond order analysis were deemed to be inappropriate with large diffuse basis sets such as these.

Bending Potential. This inquiry was initiated with the notion the complex may be bent, and as such, a discussion of efforts to locate a bent minimum structure and map the C−N−B bending potential is presented here. First of all, it was not feasible to run multiple jobs that were not constrained to C_{3v} symmetry with any basis set larger than 6-311+G*. The difference between the B−N potential energy curve for this basis set shown in Figure 3 and the curves for the larger aug-cc basis sets shown in Figure 4 makes any results from this basis set somewhat questionable. However, the argument for a bent complex lies in the mixing of orbitals to form a bond, and the shorter minimum is probably the result of partial bonding interactions. Because the 6-311+G* basis set strongly favors the shorter minimum, it should show a bent complex if one is at all favored to form. If no evidence is found of a bent complex with this basis set, then it is likely that none would be found with the larger basis sets which de-emphasize the bonding minimum. Numerous full optimizations were attempted starting from varied bent structures. Although many of the optimizations failed to converge, those that did converge returned to the C_{3v} structure. An attempt to map a potential energy surface was made by freezing several angles at set values and optimizing the remaining degrees of freedom. Most structures optimized to high-energy structures with B−N distances that were considerably longer than even the longer C_{3v} minimum. Even those structures with short B−N distances were higher in energy than the C_{3v} minimum. The resulting potential energy surface is shown in Figure 9 and gives no indication that a bent minimum exists, and the surface does not seem unusually flat. Given that this basis set overestimates the favorable energetics of the bond-forming process in this complex, it seems unlikely that a bent minimum exists.

Vibrational Frequencies. Because there is a lack of gas-phase frequencies with which to compare matrix-IR results, a comparison between the calculated frequencies for both potential minima and those measured for the crystalline and matrix isolated complexes is presented. For this analysis, the alternative assignment of ν_5 and ν_7 that was suggested in the computational study by Cho and Cheong[14] was adopted. In the solid-state study, the primary basis given for the ν_5 assignment was a comparison

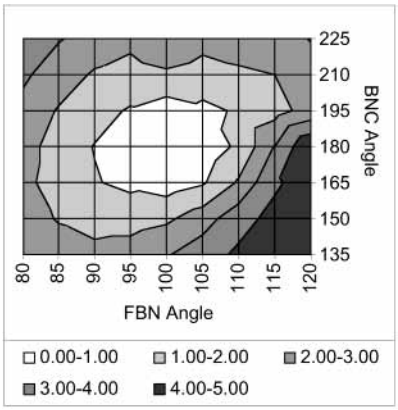

Figure 9. Potential energy surface for bending along two angular coordinates. Plot is relative energy in kcal/mol. The C_{3v} structure is at FBN = 101.7 and BNC = 180.0

to much stronger amine−BF_3 complexes. As for the ν_7 assignment, the authors relied heavily on Raman polarization data, which indicated that the 359 cm^{-1} band was A_1 symmetry, thereby distinguishing it from several other *E*−symmetry modes in that region. Because ν_5 and ν_7 are both A_1 symmetry, the Raman data would not distinguish them, and furthermore, isotope shifts measured for both bands were quite similar. Though the structural results are still not completely converged with respect to basis set, the calculated frequencies do convey how the vibrational modes depend on structure and may offer some additional insight into matrix effects. Calculated harmonic frequencies are listed in Table 2, and we note that the mode-numbering scheme is that from ref 14, rather than that from the solid-state study.[4] The general agreement between the calculated (gas phase) and solid-state frequencies is quite poor except for the modes involving motions within the methyl group. This is expected, given changes in force constants that must accompany the gas−solid structure differences (and also the geometrical distortion of the BF_3 subunit). In general, the calculated frequencies for either gas phase structure agree better with the matrix data than the crystal data, though it is at best only marginal, with the exception of ν_6 for the longer (2.3 Å) minimum structure, which is excellent, and most likely fortuitous. At first glance, the ν_{13} and ν_2 modes agree somewhat more favorably with the 1.919 Å frequencies, and the ν_6 and ν_7 modes agree with the 2.315 Å frequencies, and thus give no obvious indication that either minimum structure is more or less favored in the argon matrix.

However, the key to rationalizing matrix effects on the structure and bonding is the trends in the frequency shifts that parallel B−N bond compression. These are reflected by differences between the calculated frequencies at the two gas-phase minima and those measured for the crystal, which have 2.32, 1.93, and 1.64 Å B−N distances, respectively. For modes 1, 2, 4, 9, 12, 14, and 15, the frequencies are monotonically increasing with decreasing B−N distance. For modes 3, 10, 11, and 13, the frequencies are monotonically decreasing with decreasing B−N distance. Finally, for modes 6 and 7, the frequencies red shift between 2.32 Å and 1.93 Å, but blue shift between 1.93 Å and 1.64 Å. To investigate these trends, frequencies were calculated at every 0.05 Å on the B−N PES from 1.55 to 2.60 Å using B3LYP/6-311+G*. Such frequency calculations at nonequilibrium structures are not strictly valid. However, in the limit of zero mixing with the nonequilibrium coordinate (the B−N distance), the remaining coordinates (which are at equilibrium for that B−N distance) should be valid. These data (frequencies versus B−N distance) are displayed in Figures 10,

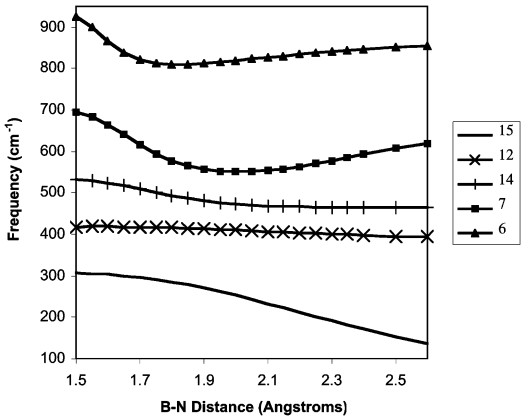

Figure 10. B3LYP/6-311+G* frequency versus B−N distance for each of the modes between 0 and 900 cm^{-1}. Mode labels are taken from Table 2.

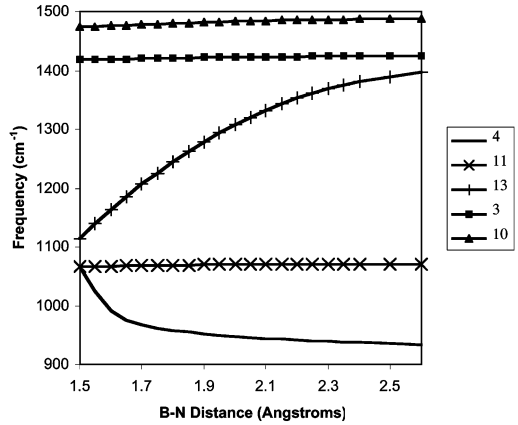

Figure 11. B3LYP/6-311+G* frequency versus B−N distance for each of the modes between 900 and 1500 cm^{-1}. Mode labels are taken from Table 2.

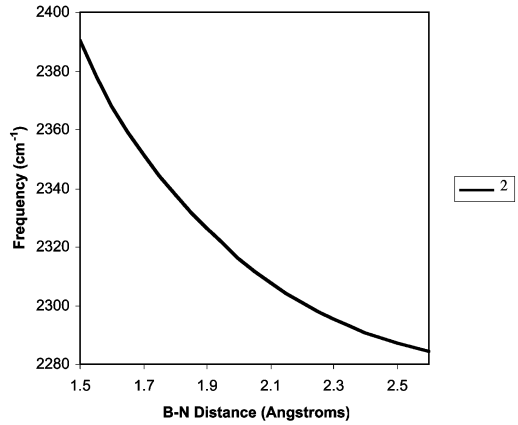

Figure 12. B3LYP/6-311+G* frequency versus B−N distance for mode 2, the nitrile stretching mode. Mode labels are taken from Table 2.

11, and 12, and for every mode, the calculations reproduce the trends noted above, *including those for the nonmonotonic ν_6 and ν_7 modes*. Given the quantitatively good agreement between experiment and theory for the frequencies of the isolated reactants, and the qualitatively accurate prediction of the trends in frequency versus bond length, it would be expected that the matrix frequencies should be better explained by the computed results. However, the matrix frequencies are not consistent with the frequency data if the experimentally determined gas-phase B−N distance of 2.011 Å is assumed. If, however, it is assumed

that the argon matrix compresses the B−N distance to a value somewhat shorter than 1.919 Å, then all four matrix frequencies are reasonably consistent with the frequency data.

This rationale is consistent with the notion that the delicate energetic balance between the two competing minima on the B−N bond potential most likely does play a key role in the medium sensitivity of the structure and bonding of CH_3CN-BF_3. Although the suggested change in (vibrationally averaged) bond length from 2.011 Å in the gas phase to less than 1.919 Å in an argon matrix seems unusual, the extremely flat B−N potential energy surface enables very small energetic effects to have a substantial impact on the B−N distance, and in turn, and other structural parameters as well (such as the N−B−F angle). In an effort to determine qualitatively whether such a bond shortening could be induced by an argon matrix, a B3LYP/aug-cc-pVQZ geometry optimization was run using the continuum dielectric CPCM model to simulate the Argon matrix.[35] The dielectric constant for liquid Argon of 1.53 at −191° was used.[36] As is often the case with SCRF calculations, tight convergence of the geometry optimization could not be achieved, but the B−N distance was converged to within 0.01 Å for 10 iterations. The B−N distance, which started at the gas-phase global minimum 2.315 Å, optimized to 1.75 Å. The complex was also optimized using the CPCM model but keeping the B−N distance frozen at 2.315 Å. This structure was found to be 1.9 kcal/mol higher in energy than the fully minimized CPCM structure. Both of these results indicate that even a very low dielectric medium can dramatically change the shape of the B−N potential energy surface in this system.

IV. Conclusions

We have examined the structure, bonding, and vibrational frequencies of the complex formed from acetonitrile and borontrifluoride using MP2, BPW91, and B3LYP computations with basis sets ranging in size from STO-3G to aug-cc-pVQZ. Both B3LYP and MP2 give similar results for this complex, so B3LYP was exclusively for analysis with the largest basis sets. Two types of equilibrium structures were found; a group with optimum B−N distances from 1.8 to 1.9 Å, and another with B−N distances from 2.2 to 2.3 Å; neither compare favorably with the experimental value of 2.011 Å.[5] The presence of diffuse functions in a basis set favors the shorter bond length structures, with the exception of the B3LYP/aug-cc-pVQZ calculation, which has an equilibrium B−N distance of 2.315 Å. The potential energy surface with respect to the B−N distance is very flat and appears to arise from two competing minima that correspond to the two groups of structures noted above. For very large basis sets with diffuse functions, aug-cc-pVTZ and aug-cc-pVQZ, the two minima are nearly isoenergetic with the triple-ζ basis set favoring the short minimum and the quadruple-ζ basis set favoring the long minimum. With these large basis sets, the overlap of the two effects leads to a very shallow potential well that remains under 0.2 kcal/mol from about 1.8 to 2.5 Å. The counterpoise correction was used to estimate the amount of basis set superposition error, and although BSSE is very small with the two large basis sets, it is sufficient to qualitatively change the global minimum from the short to the long B−N minimum for aug-cc-pVTZ and, therefore, changes the equilibrium B−N distance by 0.4 Å. Including BSSE corrections shows the calculations to be nearly converged with respect to basis set size. Zero-point energy corrections also favor the long minimum by 0.09 kcal/mol. Regardless, given the flat, asymmetric nature of the potential, it is very likely that the vibrationally averaged B−N distance differs significantly from experiment, and this may be the primary reason for the peculiar discrepancy between the experimental[5] and theoretical[11−15] structures. An AIM analysis indicates that the interaction associated with the longer, 2.3 Å minimum appears to be an electrostatic in nature, although that corresponding to the inner minimum appears to be a weak partial covalent bond. Although frontier orbital considerations suggest a possible bent minimum energy structure for the complex, no evidence of such a structure was found. Frequencies were reported for both minima with the B3LYP/aug-cc-pVQZ method, and although neither set agrees well with argon matrix experimental data, the trends in the frequency shifts that parallel B−N bond shortening suggest a B−N distance that is somewhat shorter than 1.919 Å. Thus, the computational evidence presented, both frequencies and SCRF results, suggest that even an "inert" environment such as argon may be sufficient to cause the B−N distance contract significantly.

Acknowledgement for financial support of this work is made to the Donors of the Petroleum Research Fund, administered by the American Chemical Society. This work was also supported by an award from Research Corporation, and by the Office of Research and Sponsored Programs at UWEC. We would also like to acknowledge Drs. C. Cramer and D. Truhlar for helpful discussions.

References and Notes

(1) Swanson, B.; Shiver, D. F.; Ibers, J. A. *Inorg. Chem.* **1969**, *8*, 2183.
(2) Coerver, H. J.; Curran, C. *J. Am. Chem. Soc.* **1958**, *80*, 3522. (b) Purcell, K. F.; Drago, R. S. *J. Am. Chem. Soc.* **1966**, *88*, 919.
(3) Beattie, I. R.; Gilson, T. *J. Chem. Soc.* **1964**, 2292.
(4) Swanson, B.; Shriver, D. F. *Inorg. Chem.* **1970**, *6*, 1406.
(5) Dvorak, M. A.; Ford, R. S.; Suenram, R. D.; Lovas, F. J.; Leopold, K. R. *J. Am. Chem. Soc.* **1992**, *114*, 108.
(6) Fujiang, D.; Fowler, P. W.; Legon, A. C. *J. Chem. Soc., Chem. Commun.* **1995**, 113.
(7) Janda, K. C.; Bernstien, L. S.; Steed, J. M.; Novick, S. E.; Klemperer, W. *J. Am. Chem. Soc.* **1978**, *100*, 8074.
(8) Leopold, K. R.; Fraser, G. T.; Klemperer, W. *J. Am. Chem. Soc.* **1984**, *106*, 897.
(9) Leopold, K. R.; Canagaratna, M.; Phillips, J. A. *Acc. Chem. Res.* **1997**, *30*, 57.
(10) Wells, N. P.; Phillips, J. A. *J. Phys. Chem. A* **2002**, *106*, 1518.
(11) Jurgens, R.; Almlöf, J. *Chem. Phys. Lett.* **1991**, *176*, 263.
(12) Jonas, V.; Frenking, G.; Reetz, M. T. *J. Am. Chem. Soc.* **1994**, *116*, 8741.
(13) Jiao, H. J.; Schleyer, P. v. R. *J. Am. Chem. Soc.* **1994**, *116*, 7429.
(14) Cho, H-.G.; Cheong, B-.S. *J. Mol. Struct. (THEOCHEM)* **2000**, *496*, 185.
(15) Mo, Y.; Gao, J. *J. Phys. Chem. A* **2001**, *105*, 6530.
(16) Kimura, K.; Katsumata, S.; Achiba, Y.; Yamazaki, T.; Iwata, S. *Handbook of HeI Photoelectron Spectra of Fundamental Organic Compounds*; Japan Scientific Society Press: Tokyo, 1981.
(17) LoBue, J. M.; Rice, J. K.; Blake, T. A.; Novick, S. E. *J. Chem. Phys.* **1986**, *85*, 4216.
(18) Phillips, J. A.; Canagaratna, M.; Goodfriend, H.; Grushow, A.; Almlöf, J.; Leopold, K. R. *J. Am. Chem. Soc.* **1995**, *117*, 12 549.
(19) Grushow, A. Ph.D. Thesis, University of Minnesota, 1994.
(20) a) Becke, A. D. *Phys. Rev. A* **1988**, *38*, 3098. (b) Becke, A. D. *J. Chem. Phys.* **1993**, *98*, 5648. (c) Stephens, P. J.; Devlin, F. J.; Chabalowski, C. F.; Frisch, M. J. *J. Phys. Chem.* **1994**, *98*, 11 623.
(21) Frisch, M. J.; Trucks, G. W.; Schlegel, H. B.; Scuseria, G. E.; Robb, M. A.; Cheeseman, J. R.; Zakrzewski, V. G.; Montgomery, J. A., Jr.; Stratmann, R. E.; Burant, J. C.; Dapprich, S.; Millam, J. M.; Daniels, A. D.; Kudin, K. N.; Strain, M. C.; Farkas, O.; Tomasi, J.; Barone, V.; Cossi, M.; Cammi, R.; Mennucci, B.; Pomelli, C.; Adamo, C.; Clifford, S.; Ochterski, J.; Petersson, G. A.; Ayala, P. Y.; Cui, Q.; Morokuma, K.; Malick, D. K.; Rabuck, A. D.; Raghavachari, K.; Foresman, J. B.; Cioslowski, J.; Ortiz, J. V.; Stefanov, B. B.; Liu, G.; Liashenko, A.; Piskorz, P.; Komaromi, I.; Gomperts, R.; Martin, R. L.; Fox, D. J.; Keith, T.; Al-Laham, M. A.; Peng, C. Y.; Nanayakkara, A.; Gonzalez, C.; Challacombe, M.; Gill, P. M. W.; Johnson, B. G.; Chen, W.; Wong, M. W.; Andres, J. L.; Head-Gordon, M.; Replogle, E. S.; Pople, J. A. *Gaussian 98*, revision A.9; Gaussian, Inc.: Pittsburgh, PA, 1998.
(22) Møller, C.; Plesset, M. S. *Phys. Rev.* **1934**, *46*, 618.

(23) Dunning, T. H., Jr. *J. Chem. Phys.* **1989**, *90*, 1007. (b) Kendall, R. A.; Dunning, T. H., Jr. *J. Chem. Phys.* **1992**, *96*, 679. (c) Davidson, E. R. *Chem. Phys. Lett.* **1996**, *220*, 514.

(24) Hehre, W. J.; Ditchfield, R.; Pople, J. A. *J. Chem. Phys.* **1972**, *56*, 2257. (b) Hariharan, P. C.; Pople, J. A. *Theo. Chim. Acta* **1973**, *28*, 213.

(25) McLean, A. D.; Chandler, G. S. *J. Chem. Phys.* **1980**, *72*, 5639. (b) Krishnan, R.; Binkley, J. S.; Seeger, R.; Pople, J. A. *J. Chem. Phys.* **1980**, *72*, 650.

(26) Boys, S. F.; Bernardi, F. *Mol. Phys.* **1970**, *19*, 553.

(27) Burke, K.; Perdew, J. P.; Wang, Y. In *Electronic Density Functional Theory: Recent Progress and New Directions*; Dobson, J. F., Vignale, G., Das, M. P., Eds.; Plenum Publishing Company: London, 1998. (b) Perdew, J. P.; Chevary, J. A.; Vosko, S. H.; Jackson, K. A.; Pederson, M. R.; Singh, D. J.; Fiolhais, C. *Phys. Rev. B* **1992**, *46*, 6671. (c) Perdew, J. P.; Burke, K.; Wang, Y. *Phys. Rev. B* **1996**, *54*, 16 533.

(28) Scott, A. P.; Radom, L. *J. Phys. Chem.* **1996**, *100*, 16 502.

(29) Vijay, A.; Sathyanarayana, D. N. *J. Phys. Chem.* **1996**, *100*, 75.

(30) Vanderryn, J. *J. Chem. Phys.* **1959**, *30*, 331.

(31) Bader, R. F. W. *Atom in Molecules−A Quantum Theory*; Oxford University Press: Oxford, 1990.

(32) Carroll, M. T.; Bader, R. F. W. *Mol. Phys.* **1988**, *65*, 695.

(33) a) Mó, O.; Yáñez, M.; Elguero, J. *J. Chem. Phys.* **1992**, *97*, 6628. (b) Popelier, P. L. A.; Bader, R. F. W. *Chem. Phys. Lett.* **1992**, *189*, 542. (c) Mó, O.; Yáñez, M.; Elguero, J. *J. Mol. Struct. (THEOCHEM)* **1994**, *314*, 73.

(34) Leopold, K. R. In *Advances in Molecular Structure Research*; Hargittai M., Hargittai I., Eds.; JAI Press: Greenwich Connecticut, 1996; Vol 2, p 103.

(35) a) Miertus, S.; Scrocco, E.; Tomasi, J. *Chem. Phys.* **1981**, *55*, 117. (b) Barone, V.; Cossi, M. *J. Phys. Chem. A* **1998**, *102*, 1995.

(36) *CRC Handbook of Chemistry and Physics*; 71st ed.; Lide, D. R., Ed.; CRC Press: Boca Raton, USA, 1990